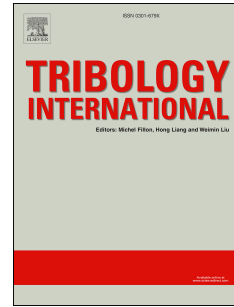# Accepted Manuscript

Transfer film formation mechanism and tribochemistry evolution of a low-wear polyimide/mesoporous silica nanocomposite in dry sliding against bearing steel

Jian Ma, Xiaowen Qi, Yu Dong, Yuanliang Zhao, Qinglong Zhang, Bingli Fan, Yulin Yang

Please cite this article as: Ma J, Qi X, Dong Y, Zhao Y, Zhang Q, Fan B, Yang Y, Transfer film formation mechanism and tribochemistry evolution of a low-wear polyimide/mesoporous silica nanocomposite in dry sliding against bearing steel, *Tribology International* (2018), doi: 10.1016/j.triboint.2017.12.026.

Transfer film formation mechanism and tribochemistry evolution of a low-wear polyimide/mesoporous silica nanocomposite in dry sliding against bearing steel

Jian Ma[1, 2], Xiaowen Qi[1, 2,*], Yu Dong[3], Yuanliang Zhao[1, 2], Qinglong Zhang[1, 2], Bingli Fan[1, 2], Yulin Yang[1, 2,*]

[1]School of Mechanical Engineering, Yanshan University, Qinhuangdao 066004, P. R. China

[2]Aviation Key Laboratory of Science and Technology on Generic Technology of Self-Lubricating Spherical Plain Bearing, Yanshan University, Qinhuangdao 066004, P. R. China

[3]Department of Mechanical Engineering; School of Civil and Mechanical Engineering, Curtin University, Perth, WA 6845, Australia

Abstract: The addition of a kind of mesoporous silica (MPS) can significantly reduce the wear rate of a thermoplastic polyimide (PI) by more than 90%, which is ascribed to the quick formation of high-quality transfer films induced by unique tribochemical reactions [1]. In-situ observation illustrated the morphology evolution of the transfer films. Further X-ray photoelectron spectroscopy on these transfer films revealed the variation of tribochemical reactions intensity while significant tribochemically induced polymer decomposition and reactions was detected by infrared spectroscopy. Intact and robust transfer films were formed by initial tribochemical adhesion of wear debris and its subsequent accumulation and expansion on the steel surface, which was ascribed to the combined effects of tribochemistry and reduced size and varied morphology of the wear debris.

Keywords: polymer matrix composites (PMCs); friction and wear; transfer film formation; tribochemistry; XPS; ATR-IR

1. Introduction

Polyimide (PI) is a very popular and widely used engineering plastic owing to its excellent thermostability, mechanical and chemical properties in industrial applications such as relative-movement devices [2-5]. In a dry sliding process against a metal, large PI wear debris or plates are easily sheared off because the rigidity of main chains and some are transferred on surfaces of metal counterpart, causing high friction and wear of pure PI. Such triobofilms are generally thick, lumpy and weakly bonded with metal pieces [1, 6]. The incorporation of different micro/nanofillers such as carbon fibers, glass fibers, aramid fibers, ceramics and solid lubricants has been reported to contribute to over 50% increase in the wear resistance of PI [7-9]. Pozdnyakov et al. [10, 11] revealed that C_{60} materials could significantly reduce the specific wear rate of PI/C_{60} composite coating. Nanofillers like carbon nanohorns [12], carbon nanotubes [13], nanosilias [14] improve tribological properties of PI nanocomposites with good reinforcing effect. Wang et al. [15-17] evaluated synergistic effects of organic fibers, solid lubricants and nanoparticles on tribological properties of corresponding PI composites. By this means, different PI composites can be designed by altering related specification, composition and contents of fillers to adapt various working conditions. Samyn et al. [18-20] worked on tribochemical variations of PI and PI composites at room and elevated temperatures to understand the relationship between associated tribochemical variations and tribological properties of PI composites. In-situ polymerization method was employed initially to enhance tribological properties of PI composites, but with contrary outcomes obtained, possibly induced by combined effects of approaches, reinforcing agents and interfacial design [21, 22]. Many reinforcing mechanisms [2, 6-13] were proposed to explain the reason for enhancing tribological properties of PI composites, consisting of the formation of high-quality triofilms, lubricity and preferential load bearing of fillers, as well as enhanced mechanical properties. Within diverse mechanisms, the improved quality of transfer films consistently gives rise to the improvement of tribological properties of PI composites.

It is well recognized by the research community that triofilms can make great contributions to control the

*Corresponding author: Prof. X.W. Qi (qxw_tougao@163.com), Prof. Y.L. Yang (y.yang@ysu.edu.cn)

friction and wear of polymer matrix composites (PMCs) [23-25], making the investigation of the formation mechanism and morphology evolution of transfer films critical in the intensive study of polymer-metal rubbing systems. Ye et al. [26] carried out an in-situ observation of transfer film evolution based on an ultra-low wear polytetrafluoroethylene (PTFE)/Al_2O_3 composite system, which indicated a complex interaction involving transfer film adhesion, tribochemistry, wear debris morphology and mechanical responses of polymer matrices. Subsequent studies on this ultra-low wear system further revealed dominant role of mechanochemistry and nanoscale functionality from microscale Al_2O_3 fillers on the formation of robust transfer film and the ultra-low wear of this material system [27-28]. Bahadur and Sunkara [29] quantitatively measured the bonding strengths between polyphenylene sulfide (PPS) nanocomposite transfer film and steel substrate. A proportional relationship was determined between such bonding strengths and wear resistance of nanocomposites. Chang et al. [30] correlated layer thickness of transfer films with tribological properties of polymer composites as a function of transfer film efficiency factor so that the friction and wear of the sliding system could be analyzed, resulting in a Stribeck type diagram. Nevertheless, while improved transfer film quality has been explained as one major reason for the enhancement of triobological properties of PI-matrix composites [1, 2, 6-10], the transfer film formation mechanism of PI-matrix composites still remains neglected. In most cases, transfer films are regarded as a consequence of tribological behavior and studies considering the formation and evolution of the transfer film as a process of tribological behavior are rarely found.

Our previous work [1, 31] demonstrated excellent wear resistance of PI/MPS nanocomposites and the reinforcing mechanism arose from improved-quality transfer films induced by tribochemical reactions between mesoporous silica (MPS) and PI molecules. However, formation mechanism of such critical transfer film as well as accompanying tribochemistry evolution remain mysterious. In this paper, we tried to shed light and to make a conceptual framework on this issue. An in-situ observation approach was applied to observe the morphology evolution of the transfer films. X-ray photoelectron spectroscopy (XPS) and Attenuated total reflectance-infrared spectroscopy (ATR-IR) analysis were employed to further explore the tribochemically induced polymer decomposition and reaction. Moreover, the key contribution from tribochemical reactions during the initial run-in stage as to the formation of high quality transfer films was revealed.

2. Experimental

2.1. Materials

PI was synthesized using tetracarboxydiphthalic ether dianhydride (ODPA) and 4,4′-diaminodiphenyl ether (ODA) as monomers via chemical imidization [1, 22]. MPS was synthesized using tetraethoxysilane (TEOS) as the silica source along with octylamine (OA) as template in weak acid deionized water [1]. PI/MPS nanocomposites containing 1.5 wt.% MPS were prepared using a vacuum hot press with the molding pressure of 20 MPa at the heating temperature of 370°C for the dwelling time of 1 h. GCr15 steel plates (AISI 52100) with the surface roughness of 0.1 μm were used as metal counterparts.

2.2. Tribological experiments

Linearly reciprocating pin-on-flat sliding wear tests were conducted using an Anton Paar Tribometer with reciprocating friction stroke of 8 mm and reciprocating frequency of 3 Hz under normal load of 10 N under room-temperature environment, which followed the recommendations of ASTM G133-05 with slightly varied parameters to match the tribometer. The linearly reciprocating wear schematic diagram was present in Fig. 1. The transfer film would be formed on the steel surface after wear test, which is convenient for subsequent observation and analysis. PI/MPS nanocomposites was cut into pins with a diameter of ~1 mm, which produces a contact pressure of 12.8 MPa. Pin surface was prepolished using 2000 grit silicon carbide sandpapers. Prior to wear tests, a sliding distance of 0.5 m under a normal load of 1 N for the PI/MPS nanocomposites pins was set up to achieve an even pressure distribution in wear tests. GCr15 steel plates were used as metal sliding counterparts. Both pins and

steel plates were cleaned with acetone prior to wear tests. The morphology evolution of transfer films were analyzed by periodically interrupting the wear tests. The coefficient of friction (COF) and associated COF curves were recorded by the tribometer.

It is noted that the wear loss of the PI/MPS nanocomposites was so little that it cannot be accurately measured using a balance with a resolution of 0.00001 g until 30 m of sliding. This is unacceptable in order to demonstrate the wear feature of the composites. Consequently, wear characteristics of PI/MPS nanocomposites in dry sliding against bearing steel was inspected by means of the "penetration depth" which was online-recorded by the tribometer equiped with a high accuracy angular sensor. Penetration depth indicates the vertical displacement of PI/MPS nanocomposites pin and can act as good indicator of wear characteristics of the PI/MPS nanocomposites. Similar parameter, vertical displacement, was frequently used in polymer tribology [20, 32]. It is worth noting that the penetration depth is not equal with the accurate wear loss of the PI/MPS nanocomposites, but reflects the wear characteristics of the nanocomposites. Repeated wear test results were presented in Section 3.1 to show the consistency and reliability of the penetration depth. Each test was repeated by at least three times to ensure test reproducibility.
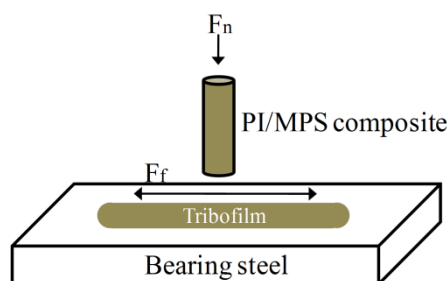

Fig. 1 Linearly reciprocating wear schematic diagram.

2.3. Characterization

Optical images of the transfer films were captured using the optical microscope within an Anton Paar Indepention. Transfer films of PI/MPS nanocomposite formed at sliding distances of 10, 41, 100, 340 and 650 m (625, 2563, 6250, 21250 and 40625 cycles) were used to investigate the evolution of tribochemical reactions via XPS analysis and XPS analysis on transfer films of pristine PI formed at sliding distances of 41, 100, and 650 m (2563, 6250 and 40625 cycles) was also performed for comparison purpose. XPS spectra on transfer films were detected using a PHI-5400 system (Perkin Elmer, U.S.A). The C1s binding energy was set to be 285 eV for the initial calibration purpose. A Phenom scanning electron microscope (SEM) device was used to capture microimages of wear debris and a Zeiss EVO18 was used to obtain the energy dispersive spectrometer (EDS) analysis of the transfer films. ATR-IR spectra on pristine PI/MPS nanocomposite and its transfer films corresponding to different sliding distances were obtained using Nicolet iN10 MX in the wavenumber rage of 4000-500 cm^{-1} with resolution of 0.4 cm^{-1}. A 100 μm^2 area within the central region of the transfer films defines the analysis area.

3. Results and discussion

3.1. Friction and wear characteristics of PI/MPS nanocomposites

COF variation and wear volume in terms of sliding distances are illustrated in Fig. 2 to demonstrate the friction and wear characteristics of the PI/MPS nanocomposites. From the primary COF curve in Fig. 2(a), frictional fluctuation and re-running in were observed after frequent interruption of wear tests, while the repeated tests yielded COF curves exhibiting general friction features of this rubbing system such as stabilization and short running-in time, signifying that such an interruption affected the friction features of PI/MPS nanocomposites. Besides, lower COF values of the interruptted wear in comparison to the repeated ones was also observed, indicating friction reduction effect of the frequent interruption. This finding coincided with the phenomenon shown in PTFE/Al$_2$O$_3$ composite systems [26]. Fig. 2(b) revealed the penetration depth variation in friction tests as fuction

of sliding distance. As shown by the primary curve, at first 50 m of sliding, slope of the penetration depth following each interruption decreased in a monotonic manner. Such feature was also observed in the repeated curves, which coincided with the frequently-referred "running-in" period also presented in the COF curves in Fig. 2(a). After this, a linear curve of the penetration depth was realized in both the primary and repeated curves, implying steady wear of the friction pair.
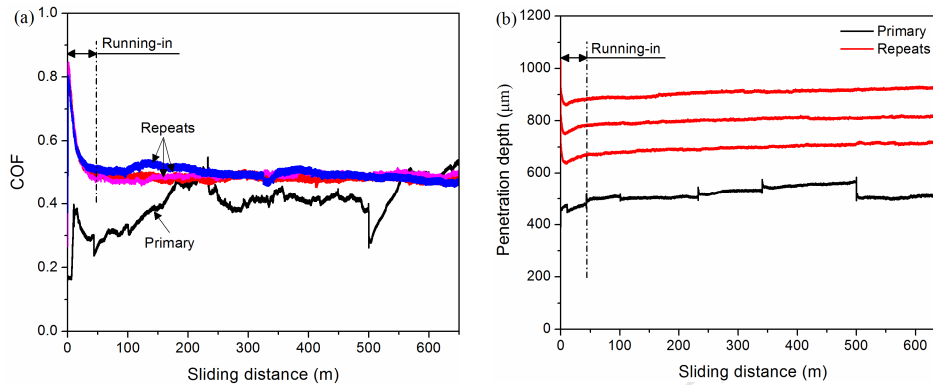

Fig. 2 COF variation (a) and penetration depth (b) of the PI/MPS nanocomposite with sliding distance.

3.2. Transfer film formation

In-situ optical images of transfer films at a single location with different sliding distances were demonstrated to reveal their morphology evolution and formation mechanism, as shown in Fig. 3. Bare steel surface was also presented in Fig. 3 for comparison purpose. It is notable that the dark area within these images indicates the transfer film. The formation of transfer film, from initial random attachments of wear debris to their further accumulation, extending and formation of an apparent layer of transfer film was clearly observed in Fig. 3. To observe the morphology evolution more intuitively, transfer films within the square area in Fig. 3 were extracted and presented in Fig. 4. The brightness and contrast of these extracted images were increased by -40% and 80% to magnify the difference between the transferred material and the original steel surface. In Fig. 4, the dark area represented the transfer film while the bright area indicated the steel surface. It can be seen that the transfer film darkened as sliding distance increased, indicating the gradual formation of the transfer film. At the sliding distance of 10 m, scattered but distinguishable wear debris was transferred to the steel surface, suggesting that the material transfer was initiated immediately after the start of the sliding. Subsequent scrutiny revealed that surface grooves resulting from the mechanical processing or surface polishing were the prior depositing area of wear debris [33]. After the sliding for 41 m, much more wear debris was transferred to the steel surface with the formation of a thin but distinct layer of transfer film, causing variation of wear characteristics of the PI/MPS nanocomposites shown in Fig. 2(b). When the sliding distance increased up to 100 m, the transfer film became more continuous. As for the sliding distance of 233 m, the accumulation of transferred materials yielded a continuous transfer film covering most steel surface, which was indicative of the initial formation of an intact transfer film. This phenomenon appeared to be more pronounced when the sliding distance increased from 340 to 650 m. Additionally, beyond the sliding distance of 500 m, transfer film morphology was evidently stabilized to form an intact transfer film. It is deduced that the formation mechanism of the transfer film is wear debris accumulation after its initial attachment.
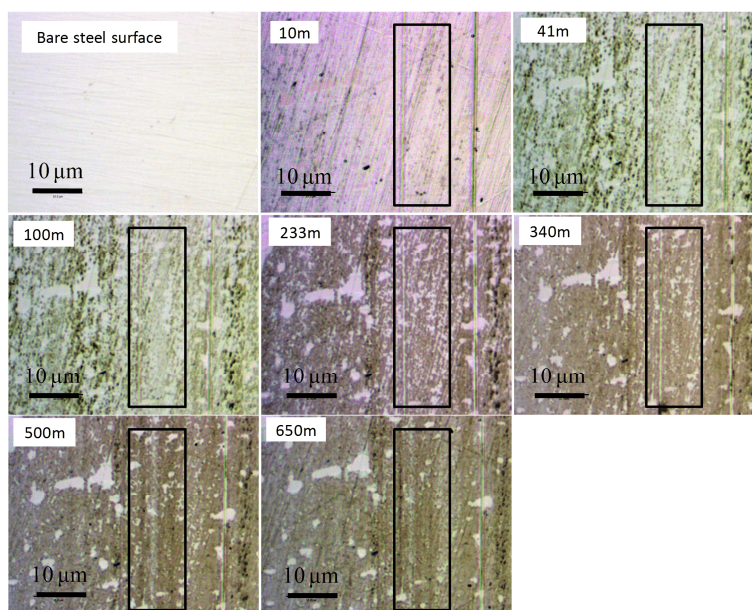
Fig. 3 Transfer film morphologies at a single location of center area of the transfer film with different sliding distances at applied laod of 10 N (12.8 MPa). Reminding that the dark area indicates the transfer films.
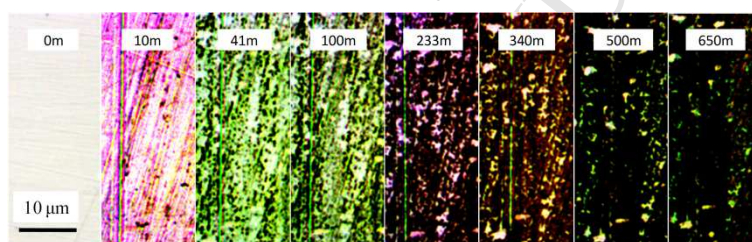

Fig. 4 Extracted transfer film morphologies revealing the morphology evolution and transfer films formation.

3.3. Tribochemistry evolution

3.3.1. XPS analysis

Our previous study demonstrates that tribochemical reactions between MPS and PI molecules play crucial role in the quick formation of uniform transfer films, as typically evidenced by the presence of Ni-Si bond in N1s XPS spectrum [1]. The tribochemical reactions by examining XPS spectra of transfer films at different sliding distances help to identify unique tribochemical features and further understand its role in the transfer film formation and low wear of PI/MPS nanocomposites. XPS survey spectra as well as C1s, N1s and Si2p spectra of transfer films and the pristine composite are depicted in Fig. 5. Particularly, intensity ratio of N-Si bond to C-N bond as function of sliding distance calculated by the area ratio of these two bonds could be used as indicator of the intensity of the tribochemical reactions, as shown in Fig. 6. For comparison, XPS spectra of transfer films of pristine PI as function of sliding distance were presented in Fig. 7. C1s and O1s peak intensities varied in Fig. 5(a) along with corresponding relative atomic contents in Table 1, which is indicative of the evolved tribochemical reactions as a function of sliding distance. More specifically, in the C1s spectra shown in Fig. 5(b), more pronounced peaks of C=C bond (284.8 eV) and C=O bond (288.4 eV) in comparison to the pristine composite were observed within the XPS spectra of the transfer films, regardless of the sliding distance. Similar variation was also observed in the case of pristine PI, as shown in Fig. 7b. Our previous study [1] and some other literatures [19, 20] suggested such variation was correlated with the structural variation of the PI molecules in friction, irrelevant with fillers. For the N1s spectra of transfer films of pristine PI shown in Fig. 7c, only C-N bond (398.4 eV) with varied intensity was detected in spectra of pristine and transfer films corresponding different sliding distances. In the case of PI/MPS nanocomposite, as shown in Fig. 5(c), only C-N bond (398.4 eV) was observed in the N1s spectra of the pristine

composite. Comparatively, both C-N bond and N-Si bond (397.4 eV) [34] were detected in the N1s XPS spectra of the transfer films formed at different sliding distances. Surprisingly, prominent N-Si bond was detected immediately after the sliding distance of 10 m in Fig. 5(c), which was intuitively proved in Fig. 6 to be the most intense tribochemical reaction. Similar variation was also detected in the Si2p spectra shown in Fig. 5(d), where only Si-O bond (103 eV) in the pristine composite and pronounced N-Si bond (102.1 eV) [34] was detected within the spectra of the transfer film at different sliding distances. Such unexpected results is contradictory to our original assumption that tribochemical reactions are a steadily strengthened process to be maximized and stabilized as soon as the friction turn into steady wear stage. However, it seemed that the tribochemical reactions between MPS and PI molecules were intensively stimulated during the initial run-in friction, as observed in Fig. 5. Since chemically attached wear debris strongly adhered to the substrate steel surface and was not easily removed by the subsequent rubbing, it is thus fated that the transfer film formation mechanism lied in the tribochemical adhesion of wear debris and its subsequent accumulation as shown via the in-situ observation of transfer film morphology.
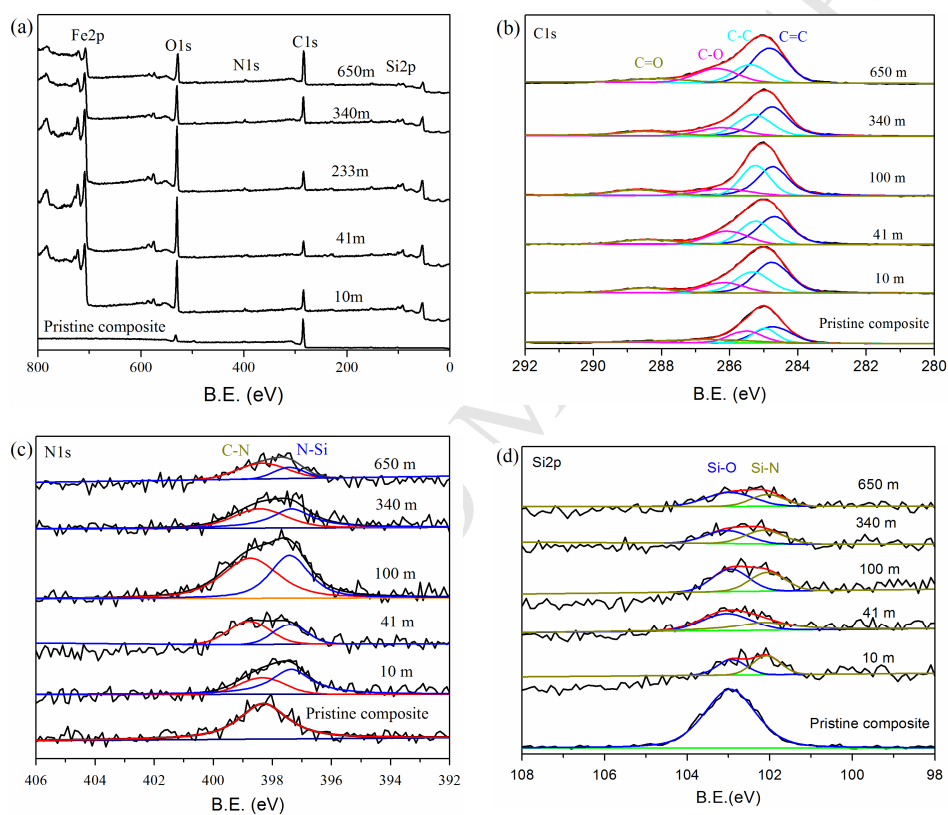

Fig. 5 (a) XPS survey spectra, (b) C1s, (c) N1s and (d) Si2p spectra of transfer films of PI/MPS nanocomposite at different sliding distances.
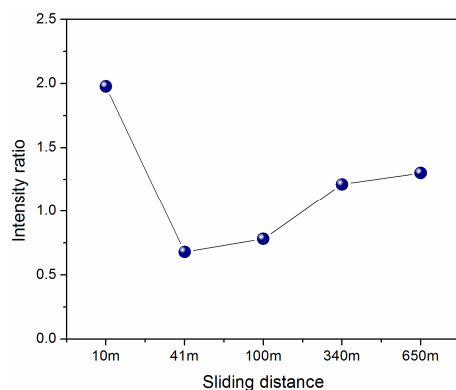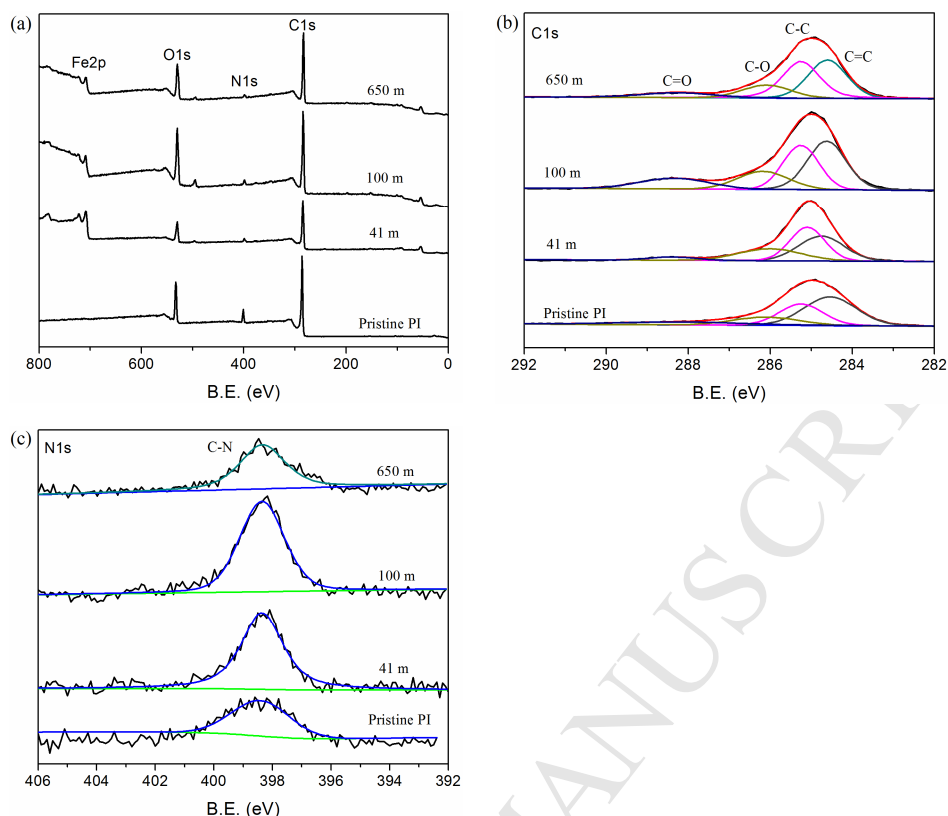
Fig. 6 Variation of intensity ratio of N-Si bond to C-N bond in N1s spectra as function of sliding distance.

Fig. 7 (a) XPS survey spectra, (b) C1s and (c) N1s spectra of transfer films of pristine PI at different sliding distances.

Table 1 Element atomic percentage (at. %) of the transfer films at different sliding distances

Elements	Atomic percentage at different sliding distances (at. %)				
	10 m	41 m	100 m	340 m	650 m
C1s	40.6	53.82	35.34	54.84	65.64
Fe2p	17.14	10.33	19.42	10.78	6.72
N1s	3.78	4.03	3.68	3.24	2.5
O1s	33.89	24.98	35.5	25.95	20.94
Si2p	4.58	6.84	6.05	5.19	4.2

3.3.2. ATR-IR analysis

ATR-IR spectra of pristine PI/MPS nanocomposites and transfer film corresponding to sliding distance of 233 m were shown in Fig. 8(a) to identify the variations between the two spectra. Typical characteristic peaks of PI, including 1238 cm^{-1} (C-O-C), 1373 cm^{-1} (C-N-C), 1500 cm^{-1} (C=C), 1720 cm^{-1} (C=O) and 1776 cm^{-1} (C=O), were observed in both spectra. Interestingly, pronounced variation was noticed in the ATR-IR spectra of the transfer film: amounts of new vibrations emerged in the wavenumber range of 3700-2000 cm^{-1} as well as in wavenumbers of 587, 1200, 1440, 1610-1620, 1659 and 1957 cm^{-1}, suggesting tribochemically induced polymer decomposition and reactions. Vibrations corresponding to these wavenumbers were listed in Table 2, according to which possible tribochemical reaction paths and products were presented in Fig. 9. The distinct detection of amide group, aromatic nitrile (C≡N), carboxylate anion (COO⁻), C≡C and carbodiimide (N=C=N) structures strongly demonstrated the decomposition of PI molecules which was attributes to the cleavage of the imide structure during the rubbing process. The appearance of Si-H bond (2150 cm^{-1}), however, indicated that the MPS was not only involved into

tribochemical reactions with the PI matrix, but also participated in other more complex tribochemical reactions. ATR-IR spectra of transfer films as function of sliding distance were separately presented in Figs. 8(b) and 8(c). At sliding distance of 10 m, despite the blurry spectra, distinguishable characteristic vibrations of PI in 1373 cm^{-1} (-C-N-C-), 2861 cm^{-1} (C-H2) and 2927 cm^{-1} (C-H3) were detected, suggesting that composite wear debris has already been transferred to the steel surface, as also revealed in Figs. 3 and 4. Moreover, vibration in 587 cm^{-1} corresponding to Fe-O bond indicated the formation of iron oxide. Strong vibration in 2150 cm^{-1} corresponding to Si-H bond implieded the deep involvement of the MPS into the tribochemical process, coincident with the XPS results (Fig. 5). Besides, the observation of vibrations in 2240 and 3185/3357 cm^{-1} respectively corresponding to C≡N and amide group indicated the decomposition of PI matrix and the generation of new activated polymer chain ends. As sliding distance increased to 41 m, new vibration around wavenumber of 1440-1460 cm^{-1} representing carboxylate anion group chelating to the steel surface firstly emerged, as circled in Fig. 8(b). When the sliding distance exceeded 100 m, as shown in Fig. 8(c), the characteristic vibrations of newly created chemical groups became more pronounced and the spectra became gradually stabilized with increasing sliding distance, indicating fully developed tribochemical reactions at long sliding distances.
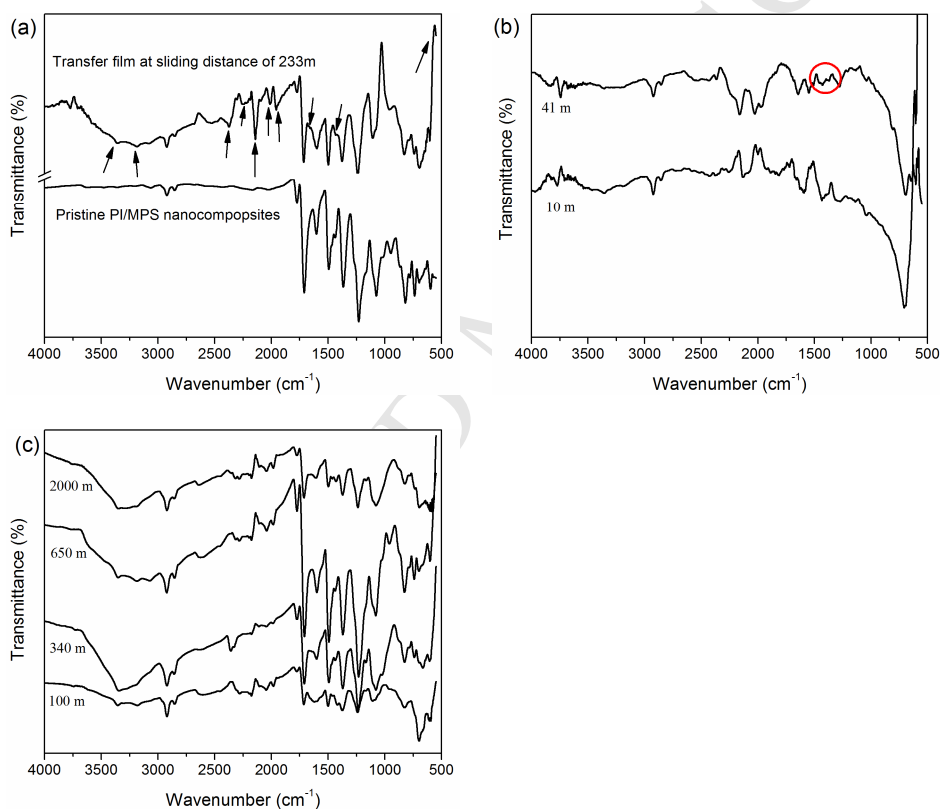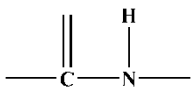

Fig. 8 ATR-FTIR spectra of a) pristine PI/MPS nanocomposites and its transfer film at sliding distance of 233 m and transfer films at sliding distances of b) 10 and 41 m and c) 100, 340 and 650 m.

Table 2 Newly created characteristic vibrations of the ATR-IR spectra of the transfer films

Vibration	Wavenumber/cm^{-1}
Fe-O	576 [35]
Si-N	1200
COO$^-$	1659/1440 [36]
COOFe C=C	1610-1620 [37]

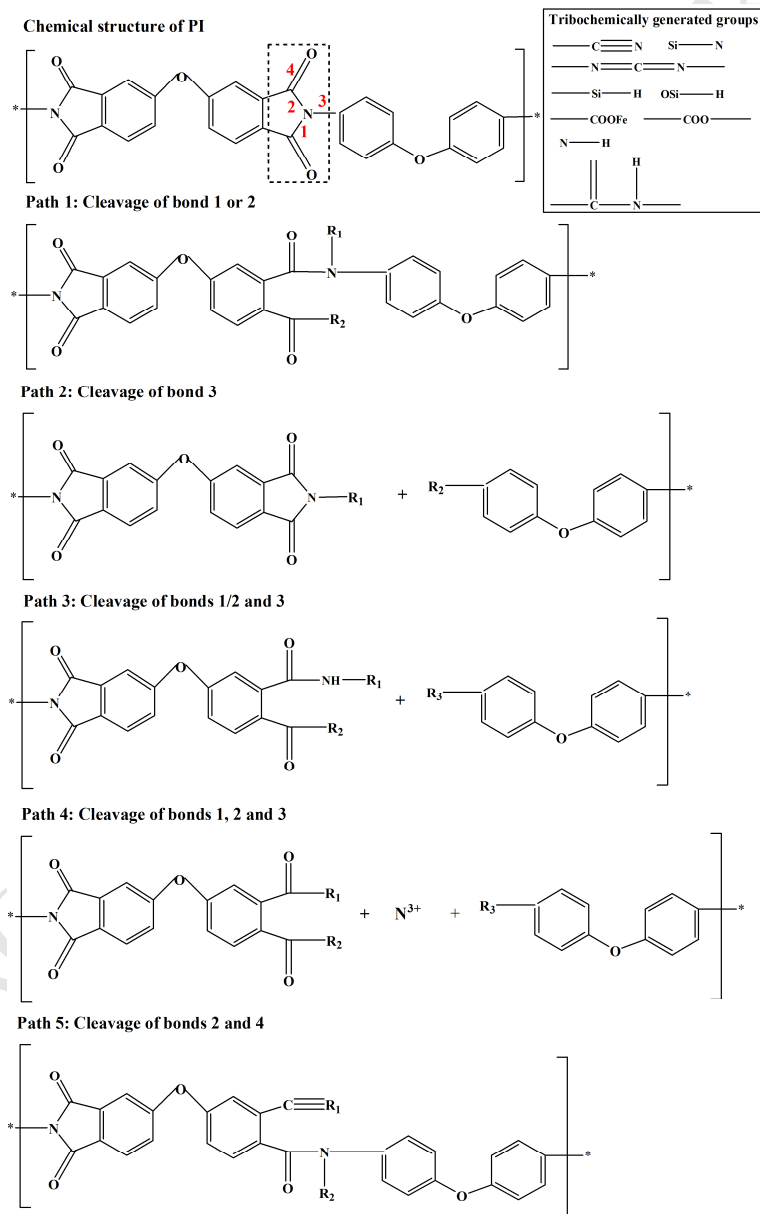|	
C=O C=C	1957
N=C=N	2004 [38]
Si-H	2150 [39]
C≡N	2240 [40]
N-H	2375 [37]
(C=O, H–N structure)	3357/3185 [38]
SiO-H	3000-3500

Fig. 9 Possible tribochemical reaction paths and products during rubbing process between PI/MPS nanocomposites and bearing steel.

3.4. Discussion

Wear results (Fig. 2b) suggested high initial wear of the PI/MPS nanocomposites. Wear during this period mainly resulted from the mechanical plough by the rigid asperities of the steel surface. The MPS additives were not expected to be influencial on the wear features of PI matrix at this stage. As sliding continued, a transition from high wear to low wear was manifested at ~50 m of sliding distance, which coincided with the formation of transfer films (Figs. 3 and 4). The gradually formed transfer film protected the nanocomposites from the mechanical plough of the rigid asperities of the steel counterpart and thus lower wear rate could be achieved.

Tribochemical reactions between PI and MPS have long been revealed by our previous study [1], while ATR-IR analysis on the transfer films in this paper further demonstrated the generation of numerous newly created chemical groups (Fig. 8 and Table 2), delivering clear message on the complexity of the tribochemical reactions. Free radicals of N and H were generated since triple bonds of -C≡N, cumulated double bonds of -N=C=N- and Si-H bond were detected in the ATR-IR spectra. In lab air, these free radicals reacted with free oxygen and water vapor to form new chemical groups as shown in Fig. 9, enriching the chemical bonds within the wear debris, which can be beneficial to the cohesion of the formed transfer films. Furthermore, vibrations corresponding to wavenumbers of 1620, 1659 and 1440 cm^{-1} represented COOFe [37], asymmetric stretching vibrations in carboxylate anion (-COO$^-$) group in bridging and bidentate forms and symmetric stretching vibrations in carboxylate anion (-COO$^-$) group in bridging form respectively [36]. Possible carboxylate configurations were shown in Fig. 10, which might be formed following the reaction paths 1, 2 and 4 shown in Fig. 9. This obervation was coincident with the detection of metal chelate salts of carboxylic acids in the case of PTFE/Al$_2$O$_3$ composites sliding against steel [27, 28]. The detection of carboxylate anion group demonstrated chemical mechanism responsible for the formation of robust transfer films, resulting in enhanced adhesion of the transfer films to the steel counterpart and the variation of sliding contact from polymer vs steel to polymer vs polymer. The formation of high-quality transfer films was reported in almost every PI-matrix composites showing good wear resistance in dry sliding against metal counterpart [2-3, 6-17]. Fundamental causes resulting in this frequently observed and reported phenomenon were never fully revealed, although some literatures reported that simple cleavage of imide group [42] or re-orientation of chemical groups of surface PI chains [20] occurred during dry sliding against steel, affecting tribological properties of PI. Research results of this paper revealed that extremely complex decomposition of PI and chemical reactions between PI, MPS and bearing steel counterpart can be triggered just by simple friction-induced shear in lab air. And this tribochemically induced decomposition of PI and the creation of numerous new polymer chain ends play vital roles in the formation of robust transfer films and dominating the friction and wear behavior of the PI/MPS nanocomposites. An interesting topic regarding the universilaty of tribochemistry in dry sliding of high wear-resistant PI-matrix composites against metal counterpart is worth investigating in the future.
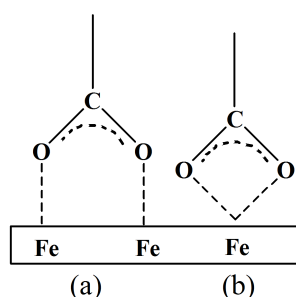

Fig. 10 Possible carboxylate configurations chelating to the steel surface: a) bridging form and b) bidentate form [41].

XPS analysis on the tribochemistry evolution (Figs. 5 and 6) revealed that the most intense tribochemical reactions between the PI and MPS were detected to be taken place at very early running-in stage. Consistently,

obvious Si-H, -C≡N and amide group detected in the ATR-IR spectra of the transfer film at 10 m of sliding distance indicated the complete decomposition of PI and activated tribochemical reactions of the PI/MPS nanocomposites and bearing steel rubbing system in initial wear stage. The evident detection of carboxylate anion (-COO⁻) group in ATR-IR spectra at sliding distance of 41 m implied the established tribochemical bonding between initially transferred wear debris and the steel surface, which was coincident with the initial formation of intact transfer films (Fig. 4) and the variation of friction and wear from running-in to steady stage (Fig. 2). This finding supported the assumption that the transfer film formation was based on the immediate tribochemical attachments of the wear debris to the steel surface, based on which intact and robust transfer films can be rapidly formed by subsequent wear debris accumulation and expansion, as observed by the morphology evolution of the transfer films (Figs. 3 and 4). At sliding distance longer than 100 m, wear debris rapidly accumulated on the steel surface to form intact transfer films at only 650 m of sliding (Fig. 4). It is assumed that the fully developed tribochemical reactions at this period (Fig. 8c) provided chemical mechanism responsible for the rapid formation of transfer films. Further EDS analysis on the transfer films generated at sliding distances of 10 m to 1000 m revealed a nearly constant Si content, as shonw in Fig. 11. This implied that MPS additives was not accumulated on the counterpart surface with increasing sliding distance, resulting in the conclusion that filler accumulation and preferential load-bearing of the MPS additives may be not responsible for the wear reduction of the nanocomposites. Another important aspect impacting the formation of transfer film lied in the wear debris size and morphology produced by the pure PI and PI/MPS nanocomposites, as presented in Fig. 12. The variation of wear debris from   micron scale solid particles to nanoscale lamellas made them more easily attaching to the counterface, which in turn helped the easy formation of transfer film. Such point of view was early proposed by Bahadur and Tabor in the study of filled PTFE [43] and also agreed by later studies [44, 45]. The greatly reduced wear debris size was also an indicator of dramastically decreased wear rate of the nanocomposites. It is then revealed that the formation of high-quality transfer film by bearing steel-PI/MPS nanocomposites rubbing system resulted from a combined effects of tribochemistry and reduced size and varied morphology of the wear debris.
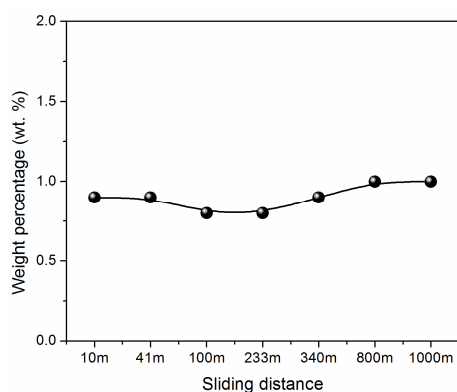

Fig. 11 Weight percentage (wt. %) of Si element within the transfer films at different sliding distances.
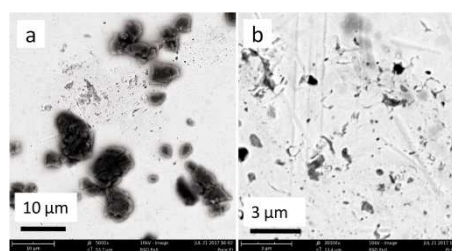

Fig. 12 Wear debris morphology and size produced by a) pure PI (magnification: 5000×) and b) PI/MPS nanocomposites (magnification: 20000×). Applied load: 10 N and reciprocation frequency: 3 Hz.

4. Conclusions

XPS and ATR-IR analysis carried out along with the in-situ observation of transfer film formation of PI/MPS nanocomposites revealed the complexity of the tribochemical process as well as the closely connection of the tribochemical process and the transfer film formation mechanism. Research results of this paper provide answers to the formation of intact and robust transfer films. The following are results obtained for the summary:

1) XPS analysis on the transfer films formed at different sliding distances suggested that the most intense

tribochemical reactions occurred during the initial run-in wear stage, which was also supported by the ATR-IR analysis.

2) A vast number of new chemical groups were detected by ATR-IR analysis on transfer films of PI/MPS nanocomposites, revealing a meaningful fact that PI is able to be decomposed and reacted with other agents by simple friction shear in lab air. More remarkably, such tribologically induced polymer decomposition can be realized in a very short sliding distance (10 m).

3) Tribochemically created new polymer chain ends within the transfer films were able to enhance the cohesion of the transfer film. The formation of carboxylate anion (-COO⁻) chelating to the steel surface in bridging form and bidentate form, which emerged as the friction and wear of PI/MPS nanocomposites transitted from running-in to steady stage, built the robustly chemical bonding responsible for the formation of intact transfer films. After 100 m of sliding, the tribochemical reactions were fully developed, providing chemical mechanism responsible for the rapid formation of intact and robust transfer films.

4) The formation mechanism of transfer film in dry sliding of PI/MPS nanocomposites against bearing steel was the tribochemical adhesion of the wear debris and its subsequent accumulation, which resulted from a combined effects of tribochemistry and reduced size and varied morphology of the wear debris.

Acknowledgement

References

[1] Ma J, Qi X, Zhao Y, Dong Y, Song L, Zhang Q, Yang Y. Polyimide/mesoporous silica nanocomposites: Characterization of mechanical and thermal properties and tribochemistry in dry sliding condition. Mater Design 2016; 108: 538-550.

[2] Wan H, Ye Y, Chen L, Zhou H. Influence of Polyfluo-Wax on the Friction and Wear Behavior of Polyimide/Epoxy Resin–Molybdenum Disulfide Bonded Solid Lubricant Coating. Tribol T 2016; 59(5): 889-895.

[3] Jia JH, Zhou HD, Gao SQ, Chen JM. A comparative investigation of the friction and wear behavior of polyimide composites under dry sliding and water-lubricated condition. Mat Sci Eng A-Struct 2003; 356(1): 48-53.

[4] Holmberg K, Mathews A. Coatings tribology: a concept, critical aspects and future directions. Thin Solid Films 1994; 253(1-2): 173-178.

[5] Burris DL, Boesl B, Bourne GR, Sawyer WG. Polymeric nanocomposites for tribological applications. Macromol Mater Eng 2007; 292(4): 387-402.

[6] Dong F, Hou G, Cao F, Yan F, Liu L, Wang J. The lubricity and reinforcement of carbon fibers in polyimide at high temperatures. Tribol Int 2016; 101, 291-300.

[7] Liu H, Li Y, Wang T, Wang Q. In situ synthesis and thermal, tribological properties of thermosetting polyimide/graphene oxide nanocomposites. J Mater Sci 2012; 47(4): 1867-1874.

[8] Satyanarayana N, Rajan KS, Sinha SK, Shen L. Carbon nanotube reinforced polyimide thin-film for high wear durability. Tribol Lett 2007; 27(2): 181-188.

[9] Jia Z, Hao C, Yan Y, Yang Y. Effects of nanoscale expanded graphite on the wear and frictional behaviors of polyimide-based composites. Wear 2015; 338: 282-287.

[10] Pozdnyakov AO, Kudryavtsev VV, Friedrich K. Sliding wear of polyimide-C_{60} composite coatings. Wear 2003; 254(5): 501-513.

[11] Pozdnyakov AO, Friedrich K, Kudryavtsev VV. Effects of thermal treatment on the wear behavior of polyimide-fullerene (C_{60}) composite coatings. J Mater Sci Lett 2001; 20(22): 2071-2075.

[12] Tanaka A, Umeda K, Yudasaka M, Suzuki M, Ohana T, Yumura M, Iijima S. Friction and wear of carbon nanohorn-containing polyimide composites. Tribol Lett 2005; 19(2): 135-142.

[13] Cai H, Yan F, Xue Q. Investigation of tribological properties of polyimide/carbon nanotube nanocomposites. Mater Sci Eng A-Struct 2004; 364(1): 94-100.

[14] Lai SQ, Li TS, Wang FD, Li XJ, Yue L. The effect of silica size on the friction and wear behaviors of polyimide/silica hybrids by sol–gel processing. Wear 2007; 262(9): 1048-1055.

[15] Wang Q, Zhang X, Pei X. Study on the synergistic effect of carbon fiber and graphite and nanoparticle on the friction and wear behavior of polyimide composites. Mater Design 2010; 31(8): 3761-3768.

[16] Zhang X, Pei X, Wang Q. Friction and wear studies of polyimide composites filled with short carbon fibers and graphite and micro SiO_2. Mater Design 2009; 30(10): 4414-4420.

[17] Song F, Wang Q, Wang T. High mechanical and tribological performance of polyimide nanocomposites reinforced by chopped carbon fibers in adverse operating conditions. Compos Sci Technol 2016; 134: 251-257.

[18] Samyn P, Schoukens G. The lubricity of graphite flake inclusions in sintered polyimides affected by chemical reactions at high temperatures. Carbon 2008; 46: 1072-1084.

[19] Samyn P, De Baets P, Van Craenenbroeck J, Verpoort F, Schoukens G. Thermal transitions in polyimide transfer under sliding against steel, investigated by Raman spectroscopy and thermal analysis. J Appl Polym Sci 2006; 101(3): 1407-1425.

[20] Samyn P, De Baets P, Van Craenenbroeck J, Verpoort F. Postmortem raman spectroscopy explaining friction and wear behavior of sintered polyimide at high temperature. J Mater Eng Perfor 2006; 15(6): 750-757.

[21] Ha HW, Choudhury A, Kamal T, Kim DH, Park SY. Effect of chemical modification of graphene on mechanical, electrical, and thermal properties of polyimide/graphene nanocomposites. ACS Appl Mater Interfaces 2012; 4(9): 4623-4630.

[22] Zhao Y, Qi X, Dong Y, Ma J, Zhang Q, Song L, Yang Y, Yang Q. Mechanical, thermal and tribological properties of polyimide/nano-SiO_2 composites synthesized using an in-situ polymerization. Tribol Int 2016; 103: 599-608.

[23] Urueña JM, Pitenis AA, Harris KL, Sawyer WG. Evolution and wear of fluoropolymer transfer films. Tribol Lett 2015;57(1): 9.

[24] Chang L, Friedrich K, Ye L. Study on the transfer film layer in sliding contact between polymer composites and steel disks using nanoindentation. J Tribol 2014; 136(2): 021602.

[25] Qi H, Li G, Zhang G, Wang T, Wang Q. Impact of counterpart materials and nanoparticles on the transfer film structures of polyimide composites. Mater Design 2016; 109: 367-377.

[26] Ye J, Khare HS, Burris DL. Transfer film evolution and its role in promoting ultra-low wear of a PTFE nanocomposite. Wear 2013; 297(1): 1095-1102.

[27] Krick BA, Pitenis AA, Harris KL, Junk CP, Sawyer WG, Brown SC, Rosenfeld HD, Kasprzak DJ, Johnson RS, Chan CD, Blackman GS. Ultralow wear fluoropolymer composites: Nanoscale functionality from microscale fillers. Tribol Int 2016; 95: 245-255.

[28] Pitenis AA, Harris KL, Junk CP, Blackman GS, Sawyer WG, Krick BA. Ultralow wear PTFE and alumina composites: it is all about tribochemistry. Tribol Lett 2015; 57(1): 4.

[29] Bahadur S, Sunkara C. Effect of transfer film structure, composition and bonding on the tribological behavior

of polyphenylene sulfide filled with nano particles of TiO_2, ZnO, CuO and SiC. Wear 2005; 258(9): 1411-1421.

[30] Chang L, Friedrich K, Ye L. Study on the transfer film layer in sliding contact between polymer composites and steel disks using nanoindentation. J Tribol 2014; 136(2): 021602.

[31] Ma J, Qi X, Zhao Y, Zhang Q, Yang Y. Effects of elevated temperature on tribological behavior of polyimide and polyimide/mesoporous silica nanocomposite in dry sliding against GCr15 steel. Wear 2017; 374: 142-151.

[32] Samyn P, Schoukens G, Verpoort F, Van Craenenbroeck J, De Baets P. Friction and wear mechanisms of sintered and thermoplastic polyimides under adhesive sliding. Macromol Mater Eng 2007; 292(5): 523-556.

[33] Voort JV, Bahadur S. The growth and bonding of transfer film and the role of CuS and PTFE in the tribological behavior of PEEK. Wear 1995; 181: 212-221.

[34] Nghiem QD, Jeon JK, Hong LY, Kim DP. Polymer derived Si–C–B–N ceramics via hydroboration from borazine derivatives and trivinylcyclotrisilazane. J Organomet Chem 2003; 688(1): 27-35.

[35] Chen Y, Dong YQ, Yan Z, Chen D, Chen Y, Wang LH. Characteristic Analysis of Fe^3O_4 Nanoparticles Modified by Oleic Acid and Undecylenic Acid. Fuller Nanotub Car N 2017; 25(6): 363-370.

[36] Przedlacki M, Kajdas C. Tribochemistry of fluorinated fluids hydroxyl groups on steel and aluminum surfaces. Tribol T 2006; 49(2): 202-214.

[37] Poling GW. Infrared studies of protective films formed by acetylenic corrosion inhibitors. J The Electrochem Soc 1967; 114(12): 1209-1214.

[38] Shriner RL, Hermann CK, Morrill TC, Curtin DY, Fuson RC. The systematic identification of organic compounds. 8th ed.Wiley; 2003.

[39] Cai D, Neyer A, Kuckuk R, Heise HM. Raman, mid-infrared, near-infrared and ultraviolet–visible spectroscopy of PDMS silicone rubber for characterization of polymer optical waveguide materials. J Mol Struct 2010; 976(1): 274-281.

[40] Shin D.H, Ko YG, Choi US, Kim WN. Design of high efficiency chelate fibers with an amine group to remove heavy metal ions and pH-related FT-IR analysis. Ind Eng Chem Res 2004; 43(9): 2060-2066.

[41] Crowell JE, Chen JG, Yates Jr JT. A vibrational study of the adsorption and decomposition of formic acid and surface formate on Al (111). J Chem Phys 1986; 85(5): 3111-3122.

[42] Lai SQ, Yue L, Li TS, Liu XJ, Lv RG. An investigation of friction and wear behaviors of polyimide/attapulgite hybrid materials. Macromol Mater Eng 2005; 290(3): 195-201.

[43] Bahadur S, Tabor D. The wear of filled polytetrafluoroethylene. Wear1984; 98: 1-13.

[44] Chen Z, Li T, Liu X, Lü R. Friction and wear mechanisms of polyamide 66/high density polyethylene blends. J Polym Sci Polym Phys 2005; 43(18): 2514-2523.

[45] Kandanur SS, Rafiee MA, Yavari F, Schrameyer M, Yu ZZ, Blanchet TA, Koratkar N. Suppression of wear in graphene polymer composites. Carbon 2012; 50(9): 3178-3183.

Research highlights

1. Formation mechanism of tribofilm is tribochemical adhesion and subsequent accumulation.
2. The most intense tribochemical reactions occur during very initial run-in stage.
3. Complex polymer decomposition produces numerous polymer chain ends.
4. Carboxylate anion chelating to the steel surface increases adhension of transfer films.
5. Fully developed tribochemical process contributes to the quick formation of transfer films.
6. Formation of high-quality tribofilm results from tribochemistry, reduced size and varied morphology of wear debris.